Research Article

Design and Construction of Capacitors with the Use of Nano-Barium Titanate's (BaTiO$_3$) Composite Materials

P. N. Nikolarakis [iD],[1] I. A. Asimakopoulos [iD],[2] and L. Zoumpoulakis [iD][2]

[1]*Laboratory "Electrical Measurements", Sector of "Industrial Electric Devices and Decision Systems", School of Electrical and Computer Engineering, National Technical University of Athens, 9-Heroon Polytechniou str., Zografou Campus, 157 73 Athens, Greece*
[2]*Laboratory Unit "Advanced and Composite Materials", Section III "Materials Science and Engineering", School of Chemical Engineering, National Technical University of Athens, 9-Heroon Polytechniou str., Zografou Campus, 157 73 Athens, Greece*

Correspondence should be addressed to I. A. Asimakopoulos; asimako.ioannis@gmail.com

The basic idea of this work, from the beginning of the laboratory work till now, is to develop innovative polymer composite materials using nanoparticles that can polarize in such a way that electrical energy can be stored. A number of thermosetting polymers have been laboratory-polymerized and then mixed with barium titanate nanoparticles, in order to develop new polymer nanocomposites. Barium titanate is a well-known dielectric material, which is used in sensors and actuators as it is a piezoelectric and ferroelectric material. In this work, we examine the storage capability between different types of such composites by creating passive filters.

1. Introduction

Nowadays, the use of capacitors with dielectrics from composite materials of polymeric matrix constitutes an important and catalytic research field in applications of electronics, power electronics, and biomedicine. The search and research of composite materials with specific dielectric and electrical characteristics are in the heart of today's technological development and innovation. Polymer-ceramic composites have been of great interest as embedded capacitor materials because they combine the processability of polymers with the desired electrical properties of ceramics. Manufacture of capacitors with composites materials for RF applications has started since 2004 by Rao and Wong who developed a novel nanostructure polymer-ceramic composite with a very high dielectric constant [1].

This article referred to the electrical and dielectric characteristics of composite materials, whose reinforced phase consists of barium titanate nanoparticles (BaTiO$_3$). The polymeric matrixes that were used in these composite materials belong to the categories of resins phenol-formaldehyde, the polyester resins, and epoxy resins. Then, passive filters were constructed with the use of the improvised capacitors. These passive filters belong to the categories of low pass, high pass,

bandpass, and bandstop filters. Finally, the cutoff frequencies and the zones of transit or excision of these filters were recorded.

1.1. Raw Materials. The composite materials that were used as dielectric materials in the construction of capacitors are as follows: Novolac with 10% BaTiO$_3$ w/w, unsaturated polyesters with 10% BaTiO$_3$ w/w, and commercial epoxy resin (CER) with 10% BaTiO$_3$ w/w [2].

1.1.1. Novolac- (NV-) BaTiO$_3$ 10% w/w. The resin of phenolformaldehyde constitutes the polymer matrix of the composite material Novolac-BaTiO$_3$ 10% w/w. Novolac resin is a phenol-formaldehyde resin and was created in our laboratory by progressive polymerization and polycondensation mechanism. The design of phenol-formaldehyde consists of the following raw materials:

(1) Phenol (chemical type: C_6H_5OH, molecular weight: 94.11 gr/mol).

(2) Solution of formaldehyde 37% v/v (chemical type: CH_2O, molecular weight: 30.03 gr/mol). The 37% v/v formaldehyde solution had the water (H_2O) as a solvent.

(3) Hydrate oxalate acid (chemical type: $C_2H_2O_4 2H_2O$, molecular weight: 127.07 gr/mol).

TABLE 1: Molar ratio of raw materials.

Polyester code	% mol of diacids/total mol			% mol Diol/total mol
	Maleic acid (M)	Adipic acid (A)	Phthalic anhydride (PA)	Ethylene glycol (EG)
$M_1A_3PA_6$	10	30	60	110
$M_3A_4PA_3$	30	40	30	110
$M_4A_4PA_2$	40	40	20	110
$M_7A_2PA_1$	70	20	10	110
M_6A_4	60	40	0	110

The solution of phenol-formaldehyde was in substoichiometric ratio: 1 mol of ethanol for 0.75 mol of formaldehyde (1 : 0.75). The nano-barium titanate ($BaTiO_3$) which contained in the NV-$BaTiO_3$ is in form of nanopowder and has got cubic crystalline phase, size of particles less than 100 nm, purity $\geq$ 99%, density: 6.08 g/mL, and true dielectric constant 150 at 25°C.

The composite material Novolac-10% $BaTiO_3$ w/w has been produced by the process of hot molding technique. According to this method, there are two different types of die molds. The first one is the "open type mold" used for resins whose hardening raw materials (resin and hardener) are in solid form and the second one is the "closed mold" used for liquid resins. Both of the above molds are made of stainless steel. The open type mold also has four aluminum parts that control the thickness of the finished specimens, so they are also 3.0 mm thick. While the molded mold has four lead caps, whose role is to seal-seal the mold so that no liquid material escapes before it is completely cured. The die molds (open or closed type) are placed inside the thermopress, which follows a particular curing program, depending on the type of polymer matrix [2, 3].

1.1.2. Unsaturated Polyesters-BaTiO₃ 10% w/w. The unsaturated polyesters with the formations $M_1A_3PA_6$, $M_3A_4PA_3$, $M_4A_4PA_2$, $M_7A_2PA_1$, and M_6A_4 constitute the polymer matrixes of the following composites materials. They have been produced by the reaction of gradual polymerization and polycondensation mechanism. The individual compounds of these unsaturated polyesters are given below:

(1) Adipic Acid (A). Molecular formula: $C_6H_{10}O_4$, molecular weight: 146.14 gr/mol, and purity greater than 99%.

(2) Maleic Acid (M). Molecular formula: $C_4H_4O_4$, molecular weight: 116.07 gr/mol, and purity greater than 99%.

(3) Phthalic Anhydride (PA). Molecular formula: $C_8H_4O_3$, molecular weight: 148.12 gr/mol, and purity greater than 97%.

(4) Ethylene Glycol (EG). Molecular formula: $C_2H_6O_2$, molecular weight: 62.07 gr/mol, and purity greater than 99.5%.

The molar ratio of each major raw material is shown in Table 1.

Before the development and curing process of the composite materials consisting of unsaturated polyesters and 10% w/w $BaTiO_3$, via hot molding technique, chain polymerization of the unsaturated polyesters through free radical mechanism took place. In conclusion, the nano-barium titanate ($BaTiO_3$) contained in these composite materials is in the form of nanopowder and it is similar to what is used for the composition of NV-$BaTiO_3$ [3].

1.1.3. Commercial Epoxy Resin (CER) and Commercial Unsaturated Polyester (CUP) and 10% BaTiO₃ w/w. The composite material CER-BT consists of the commercial epoxy resin named Epoxol 2874, which consists of the following components: Component A (resin) and Component B (hardener). The composite material CUP-BT consists of the commercial unsaturated polyester (CUP) and 10% $BaTiO_3$ w/w. Also, the method of hot molding technique took place for the composition and hardening of these composite materials with 10% $BaTiO_3$ w/w [4].

1.1.4. Nano-Barium Titanate (BaTiO₃). The presence of $BaTiO_3$ nano-particles in this type of polyester polymer composites adds to the materials' system performance piezoelectric, ferroelectric, and pyroelectric properties. These properties can be exploited in developing "intelligent" or "smart" materials. Intelligence, at its most basic level in materials, is characterized by three fundamental functions associated with sensing, actuation, and control. These fundamental functions are also related to energy conversion mechanisms and information-transfer mechanisms which involve essential concepts at the atomic and molecular levels. Barium titanate is a wide band gap semiconductive ferroelectric material with perovskite structure which has been of practical importance for over 60 years due to its specific electrical properties. Barium titanate's great significance is expressed in its applications, which include ceramic capacitors, PTCR thermistors (positive temperature coefficient resistors/thermistors, or posistors), piezoelectric sensors, optoelectronic devices, transducers, and actuators. Furthermore, it is being applied as a capacitive material in dynamic random access memories (DRAM) in integrated circuits [3].

2. Design and Construction of Capacitors by Composite Materials

The design of the capacitors, which have been developed, is shown in Figure 1 (dimensions are in cm). The dielectric material is each of the composite materials containing 10% w/w $BaTiO_3$. In Figure 1 (dimensions are in cm), the Façade
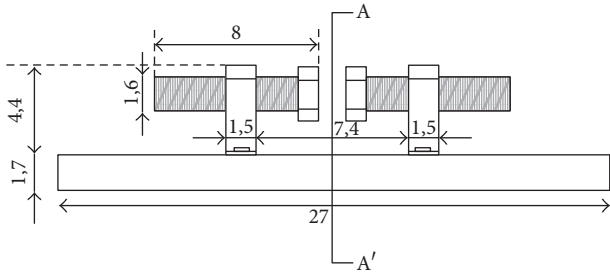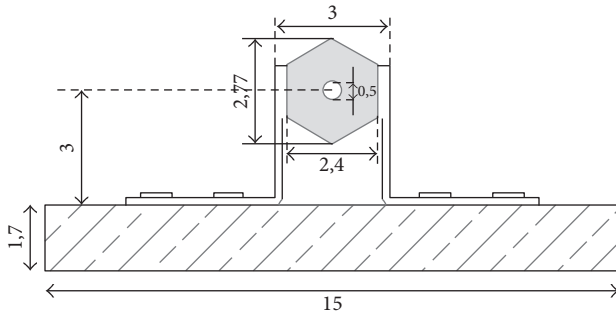
FIGURE 1: Façade.

FIGURE 2: Incision.

TABLE 2: Dimensions of the composite materials and the copper sheets.

Item of composite material	Dimensions of composite materials $[X \cdot Y \cdot Z]$ (mm)	Dimensions of the reinforcements of each capacitor (mm)
NV-BT	$19 \times 17 \times 3.0$	12×10.5
$M_1A_3PA_6$-BT	$24 \times 17 \times 3.0$	18×14
$M_7A_2PA_1$-BT	$23 \times 17 \times 3.13$	
$M_3A_4PA_2$-BT	$16 \times 17 \times 3.09$	13.5×12
$M_4A_2PA_2$-BT	$19 \times 17 \times 3.01$	
M_6A_2-BT	$16 \times 11 \times 3.0$	13×7
CUP-BT	$16 \times 13 \times 3.0$	
CER-BT	$18.5 \times 16 \times 2.90$	15×13

FIGURE 3: Right side of the capacitor.

of the capacitors is given while, in Figure 2 (dimensions are in cm), the incision of these is shown. The main building blocks of these capacitors are the wooden base, the PVC screws, and the metallic stainless steel supports for the proper compression of dielectrics. The choice of PVC screws is recommended for the nonconductive contact with the reinforcements of the capacitors. The wooden base aids the insulation of the capacitors. In Figure 2, there is a horizontal hole with 0.5 cm diameter in the center of screws, in order to pass through the wires of the reinforcements. Table 2 shows the dimensions of the composites materials and the copper sheets that were used as reinforcements on each capacitor.

The dimensions of the reinforcements are smaller than the dimensions of the composite materials, so as there is no overlap of homogeneous electric field between two copper sheets [5]. The wires and reinforcements change in our device each time, depending on the dielectric-composite material.

3. Procedures of Electric Measurements

The respective reinforcements were placed each time in the measuring device that was described above. In Figures 3 and 4, the composite materials were placed in our device, so that there is no angle between the sides of the reinforcements and the composites materials. This eliminates the coating of electric field between the reinforcements.

The measurements were performed as follows: the composite materials were placed in the adjustment device and the cables were connected in the adapter of the LCR meter. The capacitance and conductance of the composite materials were measured in the range of frequency, 10 kHz to 1 MHz. For the electric measurements, the parameters that were defined in the LCR meter (Figure 5) are given below:

(1) Frequency range: analog

(2) Measured quantities: Cp and Gp (capacitance, conductance: in parallel connection)

(3) Connector of the LCR meter: 1J10l1

(4) Bandwidth of frequency: f start = 10 kHz and f stop = 1 MHz

(5) Frequency step: 10100.8 Hz

(6) Speed of the measurements: maximum speed

(7) Time between measurements: 70 ms

(8) Width of voltage: 1 V

(9) Integration factor: log(internal regulation of the instrument)

(10) In each frequency, the result was the average of 16 measurements.

All measurements were performed at ambient conditions (temperature: 20–30°C and humidity: 30 to 40%). Except the composite material Novolac-BT, the mechanical pressure, which was exerted each time in the composite materials, was the maximum from the PVC screws. This composite material is characterized with a porous structure and it has poor mechanical properties [6, 7].

4. Results and Discussion

4.1. Graphs: Capacitance (C)-Frequency (f). In Figure 6, the unsaturated polyester $M_1A_3PA_6$-BT is distinguished with the highest capacitance, in the range of frequency 10 kHz up
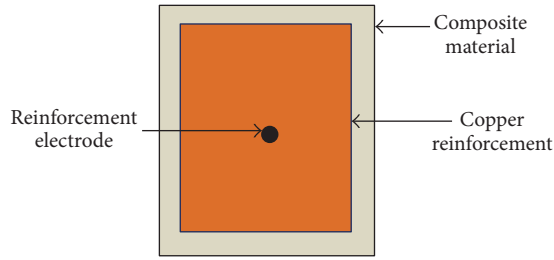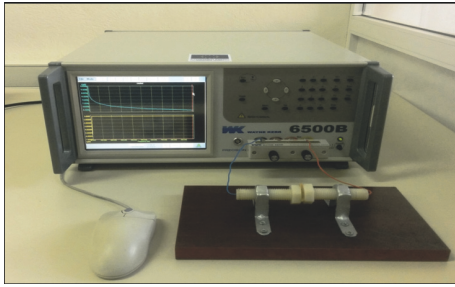
FIGURE 4: Left side of the capacitor.

FIGURE 5: Connection: capacitor-LCR instrument.

FIGURE 6: C-f graph of composite materials.

to 1 MHz. The capacitance of the commercial unsaturated polyester CUP-BT characterized with the minimum capacitance from the other unsaturated polyesters. The capacitance of the composite material CUP-BaTiO$_3$ 10% w/w (commercial unsaturated polyester-nano-barium titanate) tends to get a constant value.

The capacitor with dielectric composite material M$_1$A$_3$PA$_6$-BT 10% w/w presents higher capacitance than the capacitor with dielectric composite material M$_7$A$_2$PA$_1$-BT 10% w/w in the range of frequency, 10 kHz to 1 MHz. The first one contains six times greater amount of phthalic anhydride than the composite material M$_7$A$_2$PA$_1$-BT 10% w/w [8, 9].

The capacitance of the composite material M$_3$A$_4$PA$_3$-BT 10% w/w is higher than the capacitor with dielectric composite material M$_4$A$_4$PA$_2$-BT 10% w/w in this range of frequency. Over 50 kHz, the difference of their capacitances is almost 0.5 pF. This happens because the proportions of the initial unions which were used are similar.

Also, the capacitance of the composite material Novolac-BT 10% w/w decreases exponentially, while the frequency is increased. At frequencies greater than 50 kHz, the capacitance of this composite material presents several peaks. This happens because Novolac-BaTiO$_3$ 10% w/w is distinguished with a porous structure. Moreover, this capacitor is characterized with the lowest capacitance in this range of frequency. The capacitance of the composite material CER-BaTiO$_3$ 10% w/w includes fewer peaks compared to Novolac-BaTiO$_3$ in the range of frequency, 10 kHz to 1 MHz. This composite material is characterized with cavities on its surface.

Furthermore, the capacitance of these composite materials is reduced exponentially, while the frequency is increased.

In Figure 6, the capacitance of the capacitor with dielectric Novolac-BaTiO$_3$ has been measured with 10^{-14} sensitivity in the 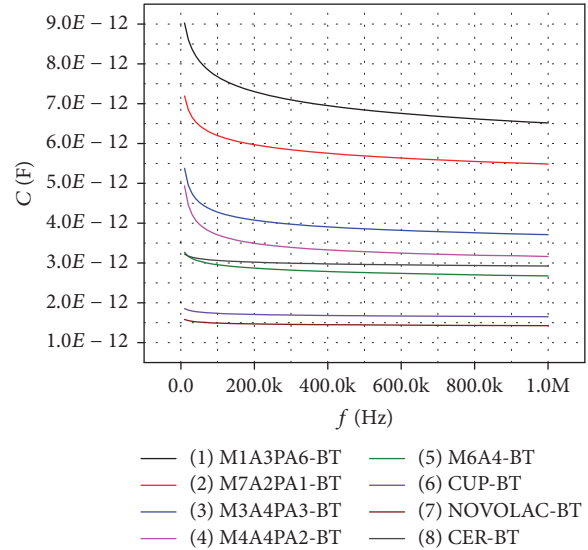range of frequency, 10 kHz to 1 MHz. There are many peaks in this chart due to the fact that this composite material has got a porous structure.

The equations which verify the capacitance of capacitors by composite materials are found by the Software OriginPro and these are the nearest equations of the straight lines or curves of capacitance of each composite material. They are given below:

(1) $y = 1{,}7468 \cdot 10^{-11} x^{-0{,}07141}$.

(2) $y = 1{,}0965 \cdot 10^{-11} x^{-0{,}05009}$.

(3) $y = 3{,}6226 \cdot 10^{-12} + 6{,}9224 \cdot 10^{-13} \cdot e^{(-x/67192{,}58)} + 1{,}2915 \cdot 10^{-12} \cdot e^{(-x/12165{,}04)} + 6{,}0588 \cdot 10^{-13} \cdot e^{(-x/530433{,}45)}$.

(4) $y = 3{,}1181 \cdot 10^{-12} + 7{,}5036 \cdot 10^{-13} \cdot e^{(-x/63917{,}8)} + 1{,}4792 \cdot 10^{-12} \cdot e^{(-x/11942{,}35)} + 5{,}5409 \cdot 10^{-13} \cdot e^{(-x/412683{,}72)}$.

(5) $y = 4{,}8692 \cdot 10^{-12} x^{-0{,}0433}$.

(6) $y = 1{,}6335 \cdot 10^{-12} + 9{,}7105 \cdot 10^{-14} \cdot e^{(-x/15495{,}82)} + 8{,}7869 \cdot 10^{-14} \cdot e^{(-x/70358{,}81)} + 9{,}4579 \cdot 10^{-14} \cdot e^{(-x/601402{,}36)}$.

(7) $y = 1{,}4141 \cdot 10^{-12} + 6{,}9058 \cdot 10^{-14} \cdot e^{(-x/11263{,}76)} + 7{,}7507 \cdot 10^{-14} \cdot e^{(-x/58596{,}58)} + 7{,}5323 \cdot 10^{-14} \cdot e^{(-x/558771{,}98)}$.

(8) $y = 2{,}8927 \cdot 10^{-12} + 1{,}5019 \cdot 10^{-13} \cdot e^{(-x/653879{,}61)} + 1{,}0252 \cdot 10^{-13} \cdot e^{(-x/111661{,}92)} + 1{,}4724 \cdot 10^{-13} \cdot e^{(-x/19511{,}3)}$.

4.2. Graphs: Conductance (G)-Frequency (f). In Figure 7, the capacitor with dielectric composite material M$_1$A$_3$PA$_6$-BaTiO$_3$ 10% w/w presents the greatest conductance in the range of frequency, 10 kHz to 1 MHz. The commercial unsaturated polyester CUP-BaTiO$_3$ 10% w/w presents the lowest conductance from the rest of unsaturated polyesters [10]. The capacitors with dielectrics composite materials M$_3$A$_4$PA$_3$-BaTiO$_3$ 10% w/w and M$_4$A$_4$PA$_2$-BaTiO$_3$ 10% w/w are characterized with similar conductance up to 300 kHz while the composite material M$_7$A$_2$PA$_1$-BaTiO$_3$ 10% w/w has got the same conductance up to 150 kHz. The composite material Novolac-BaTiO$_3$ 10% w/w is distinguished with the lowest
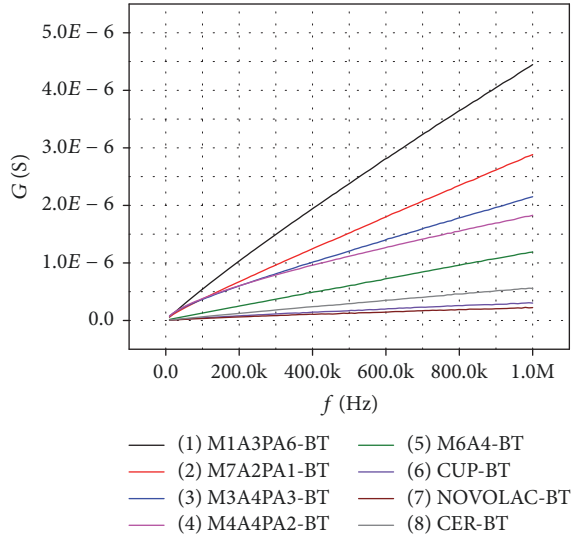
FIGURE 7: G-f graph of composite materials.

(1) M1A3PA6-BT (5) M6A4-BT
(2) M7A2PA1-BT (6) CUP-BT
(3) M3A4PA3-BT (7) NOVOLAC-BT
(4) M4A4PA2-BT (8) CER-BT

FIGURE 8: Electric circuit of low pass filter.

conductance. The composite materials CUP-BaTiO3 10% w/w and Novolac-BaTiO$_3$ 10% w/w is characterized with similar conductance up to 200 kHz.

Moreover, the conductance of all capacitors is increased exponentially, in the range of frequency 10 kHz to 1 MHz.

The equations which verify the conductance of capacitors by composite materials are found by the Software OriginPro and these are the nearest equations of the straight lines or curves of conductance of each composite material. They are given below:

(1) $y = 1{,}8903 \cdot 10^{-5} - 1{,}8856 \cdot 10^{-5} e^{(-x/3{,}7785 \cdot E6)}$.

(2) $y = 2{,}0014 \cdot 10^{-5} - 1{,}9945 \cdot 10^{-5} e^{(-x/6{,}5932 \cdot E6)}$.

(3) $y = 1{,}6109 \cdot 10^{-5} - 1{,}4918 \cdot 10^{-7} e^{(-x/69494{,}28)} - 8{,}1386 \cdot 10^{-6} e^{(-x/1{,}2245 \cdot E7)} - 7{,}7762 \cdot 10^{-6} e^{(-x/5{,}397 \cdot E6)}$.

(4) $y = 1{,}3118 \cdot 10^{-1} x^{0{,}6901}$.

(5) $y = 1{,}7165 \cdot 10^{-12} x^{0{,}9736}$.

(6) $y = 1{,}0919 \cdot 10^{-6} - 1{,}0771 \cdot 10^{-6} e^{(-x/3{,}1634 \cdot E6)} - 1{,}4186 \cdot 10^{-8} e^{(-x/69023{,}2 \cdot E6)}$.

(7) $y = 1{,}0171 \cdot 10^{-6} - 9{,}9815 \cdot 10^{-7} e^{(-x/4{,}3572 \cdot E6)} - 1{,}9488 \cdot 10^{-8} e^{(-x/98862{,}34)}$.

(8) $y = 1{,}1861 \cdot 10^{-12} x^{0{,}94645}$.

4.3. Comparative Chart of the Capacitance and Conductance of the Composites Materials.
A comparative table of the capacitance (C) and the electrical conductivity (G) in the frequency $f = 100$ KHz is given in Table 3.

We observe that, for $f = 100$ kHz, the capacitor with the dielectric-composite material $M_1A_3PA_6$-BT has the largest capacity (C) and electric conductivity (G) while the composite material with the dielectric NV-BT has got the smallest capacitance (C) and electric conductivity (G) (Table 3). This happens because the composite material $M_1A_3PA_6$-BT has got the bigger quantity of phthalic anhydride [7, 11].
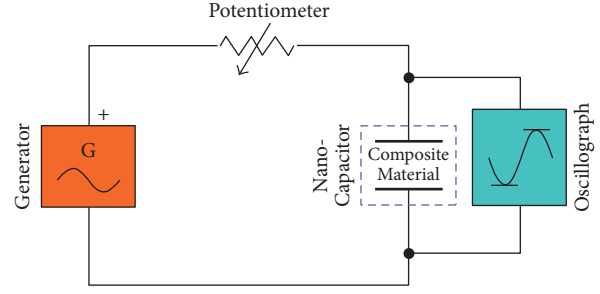
4.4. Passive Filters.
The filters, which were manufactured and described below, belong to the category of the passive filters and specifically they are as follows: low pass, high pass, bandpass, and bandstop filters. The role of the capacitor in these filters was the improvised device in which the respective composite materials were placed each time as dielectric. Then, the capacitors were connected with potentiometer that had maximum resistance 500 KΩ, on a breadboard device. For the synthesis of the bandpass and bandstop filters, we also used 20 mH inductor in parallel and serial connection, respectively. With the use of sinusoidal voltage signal Vin (Generator: Hung Chang 9205), the passive filters were powered. An oscillograph (Tektronix TBS 1052B) which was connected in parallel at the output of the filters recorded the cutoff frequencies of the low pass and high pass filters, as well as the bands of crossing or cutting of the bandpass and bandstop filters.

4.4.1. Low Pass Filters.
Figure 8 illustrated the wiring diagram of the low pass filters, in which, for each composite material that was placed in the improvised device each time, we set the value of the potentiometer, by help of a multimeter, giving specific values in the potentiometer. Specifically they are as follows: Rpoten. = 50 KΩ, 100 KΩ, and 200 KΩ [9]. Then, for each potentiometer value we changed the frequency of our generator in order to check at what frequency exactly the cutoff frequency of the filters appears. In the frequency band from 10 Hz up to 2 MHz the frequency cutoff appears when the formula below applies:

$$V\text{out} = 0.707 * V\text{in}. \tag{1}$$

The cutoff frequencies of the low pass filters are given in Table 4.

When resistance of potentiometer is $R = 500$ kΩ, then

$$V\text{out} < 0.707 \cdot V\text{in},$$
$$10\,\text{Hz} \le f \le 20\,\text{Hz}. \tag{2}$$

4.4.2. High Pass Filter.
Figure 9 illustrated the wiring diagram of the high pass filters. In these circuits, it was not observed cut-off frequency in the oscillograph. There is no frequency between 10 Hz and 2 MHz in which the below formula applies:

$$V\text{out} = 0.707 * V\text{in}. \tag{3}$$

TABLE 3: Comparative table of the capacitance (C) and the electrical conductivity (G).

$f = 100$ KHz	Capacitor $M_1A_3PA_6$-BT	Capacitor $M_7A_2PA_1$-BT	Capacitor $M_3A_4PA_3$-BT	Capacitor $M_4A_4PA_2$-BT	Capacitor M_6A_4-BT	Capacitor CUP-BT	Capacitor CER-BT	Capacitor NV-BT
C (pF)	7.67	6.19	4.27	3.703	2.95	1.74	3.062	1.491
G (S)	$5.49 \cdot 10^{-7}$	$3.77 \cdot 10^{-7}$	$3.69 \cdot 10^{-7}$	$3.83 \cdot 10^{-7}$	$1.30 \cdot 10^{-7}$	$4.47 \cdot 10^{-8}$	$6.47 \cdot 10^{-8}$	$3.41 \cdot 10^{-8}$

TABLE 4: Cuttoff frequencies of the low pass filters.

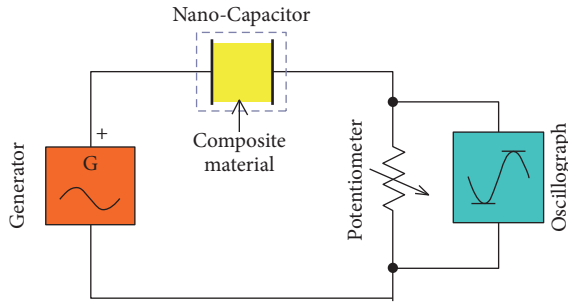| $R_{potentiometer}$ (KΩ)	Capacitor $M_1A_3PA_6$-BT	Capacitor $M_7A_2PA_1$-BT	Capacitor $M_3A_4PA_3$-BT	Capacitor $M_4A_4PA_2$-BT	Capacitor M6A4-BT	Capacitor CUP-BT	Capacitor NV-BT	Capacitor CER-BT
50	41304	61981	45808	45711	55300	55799	65607	56071
100	17288	28693	19284	19085	25179	26463	29561	26524
200	5368	12171	6108	5828	10126	10918	12956	11018

Nano-Capacitor

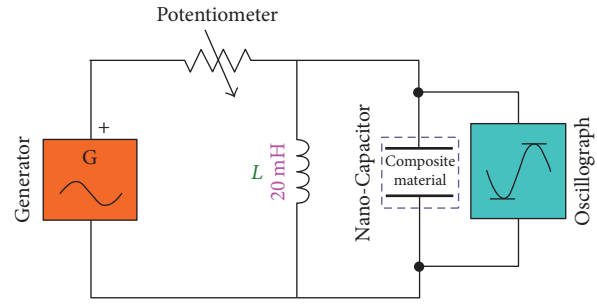FIGURE 9: Electric circuit of high pass filter.

FIGURE 10: Electric circuit of band pass filter.

This behavior of the filters is due to the fact that these capacitors are characterized by very small capacitance on the order of pF, and as a result the cutoff frequency of these filters extends beyond the generator limits ($10\,\text{Hz} \leq f_{\text{generator}} \leq 2\,\text{MHz}$).

4.4.3. Band Pass Filters. Figure 10 illustrated the wiring diagram of the band pass filters. The bandwidth of the bandpass filters is defined between the frequencies f_{C1} and f_{C2}: the output voltage Vout is equal to 0.707 of the input voltage Vin [11, 12]

$$\text{When:} \quad V\text{out} = 0.707 * V\text{in},$$
$$\text{then} \quad f = f_{C1} \tag{4}$$
$$\text{and} \quad f = f_{C2}.$$

The bandwidth of each filter is given by the formula:

$$\text{BW} = \omega_2 - \omega_1. \tag{5}$$

The formula of the quality factor of the filters is given below:

$$Q = \frac{\omega_0}{\text{BW}}, \quad \omega_0 = 2\pi f_0. \tag{6}$$

The frequencies f_{C1} and f_{C2} of the bandpass filters and the resonance frequency f_0 were measured in the oscillograph and then the quality factor of the filters was calculated. When $|V_{\text{out}}/V_{\text{in}}| = 1$ then $f = f_0$. A comparative table of the quality factor of the bandpass filters table is given in Table 5.

4.4.4. Bandstop Filters. Figure 11 illustrated the wiring diagram of the bandstop filters. These circuits do not present appropriate behavior of bandstop filters, because when the resistance of potentiometer is

(i) Rpoten. $< 100\,\text{K}\Omega$ then:

$$\text{When} \quad f \longrightarrow f_0$$
$$\text{then:} \quad \left|\frac{V_{\text{out}}}{V_{\text{in}}}\right| \neq 0. \tag{7}$$

When the frequency of the generator is near the cutoff frequency of the filter, it is observed that the sinusoidal signal pass from the circuit.
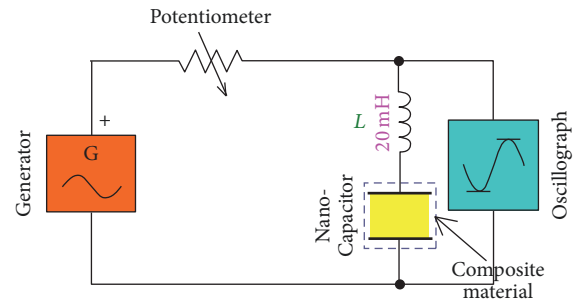

FIGURE 11: Electric circuit of bandstop filter.

(ii) Rpoten. $> 100\,\text{K}\Omega$ then:

$$\text{When} \quad f \longrightarrow f_0$$
$$\text{then:} \quad \left|\frac{V_{\text{out}}}{V_{\text{in}}}\right| < 0.707. \tag{8}$$

There is no upper frequency limit for passing the sinusoidal signal from the bandstop filter. This happens because we have a large voltage drop on the resistance of potentiometer when Rpoten. $> 100\,\text{K}\Omega$ [13].

5. Conclusions

From the composite materials of polymeric matrix that were used as dielectric materials in the construction of the capacitors and then in the design of electronic passive filters, it is observed that the capacitor with the dielectric material, the unsaturated polyester $M_1A_3PA_6$, has the highest capacity (C). In the frequency range from 10 kHz to 1 MHz this capacitor recorded capacitance values greater than the other capacitors. Also, this capacitor was featured by the highest electrical conductivity G (S). The following capacitor with higher capacitance and electrical conductivity is the capacitor with dielectric composite material $M_7A_2PA_1$-BT, in the frequency range from 1 MHz to 10 KHz. The capacitor with dielectric material NV-BT is characterized by the smallest capacitance and the lowest electrical conductivity G (S). This is due to the fact that this composite material is porous. The relative dielectric constant of this material $e_{r'}$ is the result of the dielectric constant of the composite material: $e_{r,\text{comp.}}$ material and the dielectric constant of air: $e_{r,\text{air}}$. The capacitor with

TABLE 5: Quality factor of the bandpass filter.

Rpoten. (kOhm)	Capacitor $M_1A_3PA_6$-BT	Capacitor $M_7A_2PA_1$-BT	Capacitor $M_3A_4PA_3$-BT	Capacitor $M_4A_4PA_2$-BT	Capacitor M_6A_4-BT	Capacitor CUP-BT	Capacitor CER-BT	Capacitor NV-BT
10	0.597	0.55	0.606	0.558	0.594	0.534	0.54	0.53
20	1.378	1.013	1.269	1.272	1.172	1.130	1.012	1.077
50	4.261	2.954	3.612	3.573	2.915	2.600	2.700	2.579

composite material, the commercial unsaturated polyester-barium titanate (CUP-BT), occupies the second position with the smallest capacitance and electrical conductivity [14].

At high frequencies (>900 KHz), the capacitors with dielectric materials $M_1A_3PA_6$-BT and $M_7A_2PA_1$-BT tend to take a constant value of capacitance. It happens because the dipoles, due to the inactivity, do not follow the orientation of the homogeneous electric field. The capacitors with the dielectric materials $M_3A_4PA_3$-BT and $M_4A_4PA_2$-BT acquire a constant value of capacitance in frequencies greater than 700 KHz. Also, the capacitor with the dielectric M_6A_4-BT tends to take a constant capacitance value for $f >$ 300 KHz, while the capacitor with dielectric, the commercial unsaturated polyester CUP-BT, presents an almost constant capacitance value (C) across the frequency range from 10 KHz to 1 MHz.

Finally, the capacitor with the dielectric material CER-BT has an almost constant capacitance after 600 KHz, while, for the capacitor with dielectric NV-BT, it happens after 200 KHz.

The circuits, which were designed by using the above capacitors, present behavior of cutoff filters, because of the fact that, for low frequencies, the input signal passes while, for high frequencies, the signals are cut off. By increasing the resistance value of the potentiometer, the cutoff frequency of the filters is decreased. The bandpass filters, which were designed based on these capacitors, present a good behavior as bandpass filters for values potentiometer resistance Rpoten. ≤ 50 KΩ, while, for values of resistance potentiometer $R > 50$ KΩ, it is observed that the ratio of the output voltage to the input is

$$\left| \frac{V_{OUT}}{V_{IN}} \right| < 1 \quad \text{for } f \longrightarrow f_0. \tag{9}$$

This happens because of the fact that large voltage drop is observed on the resistance of the potentiometer; as a result these circuits do not have an appropriate behavior as bandpass filters. It is also observed that the increase of potentiometer's resistance from 10 KΩ to 50 KΩ improves the quality factor Q of the bandpass filters significantly [15]. The bandpass filter with the capacitor that has as dielectric the composite material $M_1A_3PA_6$-BT presents the highest value of the quality factor. The classification of bandpass filters (RLC) based on the quality factor can be made as follows:

L = constant

(i) For Rpoten. $= 10$ KΩ is

$$Q_{RLC(M3A4PA3\text{-}BT)} > Q_{RLC(M1A3PA6\text{-}BT)} > Q_{RLC(M6A4\text{-}BT)}$$
$$> Q_{RLC(M4A4PA2\text{-}BT)}$$
$$> Q_{RLC(M7A2PA1\text{-}BT)} > Q_{RLC(CER\text{-}BT)} \tag{10}$$
$$> Q_{RLC(CUP\text{-}BT)} > Q_{RLC(V\text{-}BT)}.$$

(ii) For Rpoten. $= 20$ KΩ is

$$Q_{RLC(M1A3PA6\text{-}BT)} > Q_{RLC(M4A4PA2\text{-}BT)}$$
$$> Q_{RLC(M3A4PA3\text{-}BT)} > Q_{RLC(M6A4\text{-}BT)}$$
$$> Q_{RLC(CUP\text{-}BT)} > Q_{RLC(V\text{-}BT)}$$
$$> Q_{RLC(M7A2PA1\text{-}BT)} > Q_{RLC(CER\text{-}BT)}. \tag{11}$$

(iii) For Rpoten. $= 50$ KΩ is

$$Q_{RLC(M1A3PA6\text{-}BT)} > Q_{RLC(M3A4PA3\text{-}BT)}$$
$$> Q_{RLC(M4A4PA2\text{-}BT)}$$
$$> Q_{RLC(M7A2PA1\text{-}BT)} > Q_{RLC(M6A4\text{-}BT)} \tag{12}$$
$$> Q_{RLC(CER\text{-}BT)} > Q_{RLC(CUP\text{-}BT)}$$
$$> Q_{RLC(V\text{-}BT)}.$$

These passive filters can be applied to electronic integrated circuits, to antennas of transmitting and receiving signal and combined with active filters can be applied in power compensation systems and cutoff harmonic of electricity networks.

Conflicts of Interest

The authors declare that they have no conflicts of interest regarding the publication of this paper.

References

[1] Y. Rao and C. P. Wong, "Material characterization of a high-dielectric-constant polymer-ceramic composite for embedded capacitor for rf applications," *Journal of Applied Polymer Science*, vol. 92, no. 4, pp. 2228–2231, 2004.

[2] I. Asimakopoulos, L. Zoumpoulakis, and G. C. Psarras, "Development and characterization of a novolac resin/BaTiO 3 nanoparticles composite system," *Journal of Applied Polymer Science*, vol. 125, no. 5, pp. 3737–3744, 2012.

[3] I. A. Asimakopoulos, G. C. Psarras, and L. Zoumpoulakis, "Barium titanate/polyester resin nanocomposites: development, structure-properties relationship and energy storage capability," *Express Polymer Letters*, vol. 8, no. 9, pp. 692–707, 2014.

[4] I. A. Asimakopoulos, G. C. Psarras, and L. Zoumpoulakis, in *Proceedings of the 30th Panhellenic Conference on Solid-State Physics and Materials Science (30th SSPMS)*, p. 187, Heraklion, Crete, Greece, September 2014.

[5] Z. S. Iro, C. Subramani, and S. S. Dash, "A brief review on electrode materials for supercapacitor," *International Journal of Electrochemical Science*, vol. 11, no. 12, pp. 10628–10643, 2016.

[6] A. M. Juliet, P. Dey, and D. J. Preshiya, "Stanene/MnO$_2$ based micro-super capacitors a composite material for energy storage," *Journal of Chemical and Pharmaceutical Research*, vol. 7, pp. 811–818, 2015.

[7] I. A. Asimakopoulos, G. C. Psarras, and L. Zoumpoulakis, in *Proceedings of the 28th Panhellenic Conference on Solid State Physics and Materials Science (28th SSPMS)*, Patras, Greece, September 2012.

[8] I. A. Asimakopoulos, G. C. Psarras, and L. Zoumpoulakis, in *Proceedings of the 10th Hellenic Polymer Society Conference (10th HPSC) with International Participation*, pp. 296–298, Patras, Greece, December 2014.

[9] A. Kevin, O. Connor, and D. R. Curry, "Recent results in the development of composites for high energy density capacitors," in *Proceedings of the Power Modulator and High Voltage Conference (IPMHVC '14)*, IEEE, San Francisco, CA, USA, June 2014.

[10] E. Frackowiak, V. Khomenko, K. Jurewicz, K. Lota, and F. Béguin, "Supercapacitors based on conducting polymers/nanotubes composites," *Journal of Power Sources*, vol. 153, no. 2, pp. 413–418, 2006.

[11] G. J. H. Melvin, Q.-Q. Ni, and T. Natsuki, "Electromagnetic wave absorption properties of barium titanate/carbon nanotube hybrid nanocomposites," *Journal of Alloys and Compounds*, vol. 615, pp. 84–90, 2014.

[12] S. George and M. T. Sebastian, "Three-phase polymer-ceramic-metal composite for embedded capacitor applications," *Composites Science and Technology*, vol. 69, no. 7-8, pp. 1298–1302, 2009.

[13] S. Ju, M. Chen, H. Zhang, and Z. Zhang, "Dielectric properties1 of nanosilica/low-density polyethylene composites: the surface chemistry of nanoparticles and deep traps induced by nanoparticles," *Express Polymer Letters*, vol. 8, no. 9, pp. 682–691, 2014.

[14] O. P. Bajpai, J. B. Kamdi, M. Selvakumar, S. Ram, D. Khastgir, and S. Chattopadhyay, "Effect of surface modification of BiFeO3 on the dielectric, ferroelectric, magneto-dielectric properties of polyvinylacetate/BiFeO3 nanocomposites," *Express Polymer Letters*, vol. 8, no. 9, pp. 669–681, 2014.

[15] O. I. Negru, L. Vacareanu, and M. Grigoras, "Electrogenerated networks from poly [4-(diphenylamino)benzyl methacrylate] and their electrochromic properties," *Express Polymer Letters*, vol. 8, no. 9, pp. 647–658, 2014.